Journal of Spacecraft and Rockets

VOLUME 7 AUGUST 1970 NUMBER 8

Thermally Induced Vibrations of Long Thin-Walled Cylinders of Open Section

HAROLD P. FRISCH*
NASA Goddard Space Flight Center, Greenbelt, Md.

Recent satellites have carried long, extendable booms of the type classified as thin-walled cylinders of open section for such diverse purposes as dipole antennas, gravity-gradient stabilization booms, and electric field probes. Flight data show that several three-axis-stabilized satellites which deploy these long booms exhibit varying degrees of anomalous spacecraft body motion while exposed to direct sunlight. NASA/GSFC has hypothesized that in many cases the observed oscillations are thermally induced. This paper presents the equations which describe the coupled nonplanar transverse and torsional vibrations of such a boom when it is exposed to direct sunlight. To obtain a numerical solution, the equations are specialized to the case of a cylinder of open section having the nominal characteristics of the booms in orbit. Comparison of results with flight data shows that the hypothesis leads to conclusions consistent with the observed phenomena. The numerical examples show that the thermally induced vibration problem can be eliminated by increasing the torsional rigidity of the boom. Flight data from the Radio Astronomy Explorer Satellite (which has four 750-ft stable zippered antennas) and the Orbiting Geophysical Observatory VI (which has two 30-ft stable torsionally rigid electron probes) support this conclusion.

Nomenclature

c = specific heat of material
e_c = thermal expansion coefficient
e_s = distance between geocenter and shear center
h = wall thickness of cylinder
$(\mathbf{i},\mathbf{j},\mathbf{k})$ = basis vectors parallel to local axis system
$(\mathbf{i}_1,\mathbf{j}_1,\mathbf{k}_1)$ = basis vectors parallel to inertially fixed axis system
$q_n(z,t)$ = nth generalized thermal coordinate
r = radius of cross section
s = position coordinate around circumference of cross section
t = time coordinate
$x_n(z),y_n(z)$ = nth clamped-free beam mode
z = position coordinate along boom's longitudinal axis
$[A_n(t),B_n(t),C_n(t)]$ = generalized displacement coordinates
$[BM_x(z,t),BM_y(z,t)]$ = components of an effective thermal bending moment vector
$C_n{}^*(t)$ = generalized force
C_T,C_w = torsional and warping rigidities, respectively
E = Young's modulus of elasticity
G_s = shear modulus
I = average geometrical moment-of-inertia of cross section
I_s = mass rotational moment-of-inertia about shear-center axis
J_s = solar-radiation intensity
K_T = thermal conductivity
P = perimeter of cross section
$Q_n(z,t)$ = generalized thermal input
T_0 = steady-state mean temperature
$\tilde{T}(s,z,t)$ = absolute temperature
$T(s,z,t)$ = deviation of absolute temperature from mean
$T_n(s)$ = nth thermal mode
$T_{sc}(z,t)$ = thermal torque
$V(z,t)$ = thermal torque coefficient
$[X_2,Y_2,Z_2]$ = local axis system
$[X_1,Y_1,Z_1]$ = inertially fixed axis system
$[X(z,t),Y(z,t),z]$ = displacement coordinates relative to fixed axis system
$[X_s(z,t),Y_s(z,t),z]$ = displacement coordinates of the thermal equilibrium position relative to fixed axis system
$[\alpha_n(t),\beta_n(t),\gamma_n(t)]$ = amplitudes of nth mode in modal expansion of $[X_s(z,t),Y_s(z,t),\varphi_s(z,t)]$
α_s = absorptivity
ϵ = emissivity
ζ_x,ζ_φ = transverse and torsional damping ratios, respectively
κ,κ' = curvature components of longitudinal axis relative to $[X_2,Y_2,Z_2]$
λ_n = thermal decay constant
ρ = weight density of material

Presented at the ASME/AIAA 10th Structures, Structural Dynamics and Material Conference, New Orleans, La., April 14–16, 1969 (no paper number; published in bound volume of conference papers); submitted July 22, 1969; revision received March 27, 1970.

* Aerospace Technologist. Member AIAA.

$\sigma(s,z,t)$ = thermal stress
$\tau(s,z,t)$ = thermal shear stress
ϕ = angular amount of overlap
$\varphi(z,t)$ = torsional coordinate
$\varphi_s(z,t)$ = torsional coordinate of thermal equilibrium position
$\varphi_n(z)$ = nth torsional mode
$\psi(z,t)$ = relative sun orientation
$\omega_{x_n},\omega_{\varphi_n}$ = nth natural bending and torsional frequencies
$\Upsilon(s,z,t)$ = function defining heat input

Introduction

NEARLY all satellites in orbit which have long extendable appendages (referred to here as booms) use the basic Storable Tubular Extendable Member (STEM) principle shown in Fig. 1. These booms have been used on Orbiting Geophysical Observatories (OGO) IV, V, and VI as electric field probes, on Department of Defense Gravity Experiment (DODGE), Applications Technological Satellite (ATS), and Gravity-Gradient Stabilization Experiment (GGSE) III, V, and VI as gravity-gradient stabilization booms, and on Radio-Astronomy Explorer (RAE) to form a large V-shaped antenna for radio-frequency (RF) reception.

The completely deployed boom may be modeled for the purposes of analysis as a clamped-free, thin-walled cylinder of open section. Its length is arbitrary, but in practice it is usually between 30–100 ft.

The phenomenon of thermally induced vibrations is shown most clearly in data obtained from the OGO-IV spacecraft. While the 60-ft electron probe is in solar eclipse, all noticeable satellite motion is rapidly damped out. However, whenever the satellite leaves eclipse and enters into full sunlight, the control system experiences a strong periodic disturbance, large enough to cause the error signal of the attitude control jets to exceed the dead band limits and result in a large expenditure of gas. The disturbance torque has the same frequency as the boom-spacecraft system and a magnitude which corresponds to that which would be produced by the boom if it were vibrating with an amplitude of about ± 20 ft.

NASA/GSFC has theorized that the observed vibrations are thermally induced. The NASA theory was the subject of a session at the Symposium on Gravity-Gradient Attitude Control.[1] The general conclusion was that this theory correctly pinpoints the cause of the anomalous motion observed on OGO IV and several other three-axis-stabilized satellites deploying booms of the type shown in Fig. 1.

The physical concept behind the theory is as follows: When a cylinder of open section is deployed in direct sunlight, thermal gradients are built up around and along it, at a rate determined by the thermal characteristics of the boom material. The boom would experience thermal stresses if it were rigidly held; as it is free, it relieves the thermal stresses by bending and twisting toward its instantaneous thermal equilibrium shape. Due to its mass inertia, this response takes time. As it twists in the directional thermal field established by the sun a change in the heat flow around the perimeter occurs. This causes a change in the over-all temperature distribution and hence a change in the position of thermal equilibrium toward which the boom is moving. It is shown that under a broad range of conditions the position of thermal equilibrium can change with a strong component at the first natural bending frequency of the boom. The system is then in effect driven at resonance and large-amplitude thermally induced bending motion can occur.

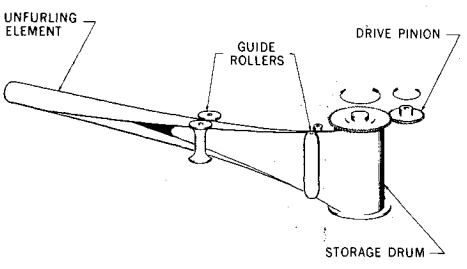

Fig. 1 The 'STEM' principle.

The purpose of this paper is to present a general method for studying the thermoelastic response of a thin-walled cylinder of either open, zippered, or closed section. The derived equations are applied to an open-section cylinder having the nominal geometric and physical characteristics of particular booms in orbit. For these examples, large-amplitude thermally induced vibration is to be expected. By increasing the boom's torsional rigidity to that of a zippered-section tube (which is close to that of a closed-section tube), the danger of thermally induced vibrations can be eliminated.

Basic Assumptions

Because of unavoidable nonuniformities in all presently manufactured flight-quality booms, experimentally determined values of stiffness, damping, and thermal characteristics show a considerable scatter. There is thus no point in an overly refined analysis. We start out with the following set of simplifying assumptions. 1) The vibrational response under a time varying thermal load can be determined by applying the techniques of elementary strength of materials described by Boley.[2] 2) The boom may be modeled as a uniform continuous thin-walled cylinder of open section having the standard linear bending and torsional stiffness characteristics described by Timoshenko.[3] 3) Bending stiffness is assumed equal about both cross-sectional principal axes of inertia. Coupling of bending and torsion due to the noncoincidence of the axis of shear centers and the axis of centroids is assumed negligible. 4) Heat flow along the boom's length and temperature gradients through the wall thickness is assumed to be negligible. 5) Heat flow around the perimeter of the cross section at any thermal station along the boom is defined by the linear equation of heat conduction and radiation in a one-dimensional solid. 6) Heat transfer across the interior of the cylinder is assumed to be negligible; however, heat transfer between overlapping surfaces is approximated by a radiation term because no smooth flush contact exists between them. 7) Energy dissipation is assumed to be describable by two independent linear viscous damping coefficients, one to define the damping of transverse motion and the other to define the damping of torsional motion. 8) The sun is assumed normal to the boom's longitudinal axis and to provide the only source of disturbance.

Thermal Loading

The time varying nonuniform temperature distribution $\tilde{T}(s,z,t)$ induces a thermal strain along the boom's length. Boley[2] and Frisch[4] state that the thermal stress $\sigma(s,z,t)$ in any fiber passing through an arbitrary cross section (see Fig. 2) can be approximated by

$$\sigma(s,z,t) = Ee_c[\tilde{T}_m(z,t) - \tilde{T}(s,z,t)] - [BM_y(z,t)/I_y]x_c(s) + [BM_x(z,t)/I_x]y_c(s) \quad (1)$$

where

$$\tilde{T}_m(z,t) = \frac{1}{P}\int_0^P \tilde{T}(s,z,t)ds \quad (2)$$

$$BM_x(z,t) = e_cEh\int_0^P \tilde{T}(s,z,t)y_c(s)ds \quad (3)$$

$$BM_y(z,t) = -e_cEh\int_0^P \tilde{T}(s,z,t)x_c(s)ds \quad (4)$$

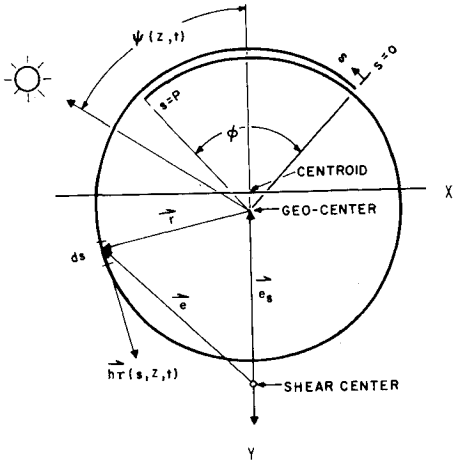

Fig. 2 Cross section of boom at thermal station z and time t.

$$I_x = h\int_0^P y_c^2(s)ds \tag{5}$$

$$I_y = h\int_0^P x_c^2(s)ds \tag{6}$$

and e_c = thermal expansion coefficient, h = wall thickness of cylinder, E = Young's modulus of elasticity, P = perimeter of cross section, $[x_c(s),y_c(s)]$ are the coordinates of the point s on the cross section relative to the cross-sectional principal axes of inertia, and the quantities $[BM_x(z,t), BM_y(z,t)]$ are referred to as the components of the effective thermal bending-moment vector at (z,t). Temperature variations along the rod's length can induce thermal shear stresses in the thin-walled cylinder.

A thermal shear flow $h\tau(s,z,t)$ has the integrated effect of producing a thermal torque. From the equilibrium equation for a thin-walled beam, namely

$$\partial h\tau(s,z,t)/\partial s = -h\partial\sigma(s,z,t)/\partial z \tag{7}$$

and the condition that the shear flow be zero along the seam, Frisch[4] shows that if the sun's rays remain nearly normal to the boom's longitudinal axis the thermal torque $T_{sc}(z,t)$ is

$$\mathbf{T}_{sc}(z,t) = -\int_0^P \mathbf{e}\times\mathbf{h\tau}(s,z,t)ds = hEe_c r\frac{\partial V(z,t)}{\partial\psi(z,t)}\frac{\partial\psi(z,t)}{\partial\varphi(z,t)}\frac{\partial\varphi(z,t)}{\partial z}\mathbf{k} \tag{8}$$

where $\mathbf{k}$ = unit vector normal to cross section at (z,t), $\mathbf{e}$ = vector connecting the shear center to the surface element ds (see Fig. 2), e_s = distance between geocenter and shear center of cross section, $\psi(z,t)$ = relative sun orientation at (z,t), and $\varphi(z,t)$ = angular amount through which the cross section at (z,t) has rotated

$$V(z,t) = \left[e_s\sin\frac{\phi}{2}+\frac{P}{2}\right]\int_0^P \tilde{T}(s,z,t)ds - \int_0^P\left[\frac{e_s}{r}\cos\left(\frac{s}{r}-\frac{\phi}{2}\right)+1\right]\int_0^s \tilde{T}(\xi,z,t)d\xi ds \tag{9}$$

From these equations, after determining $\tilde{T}(s,z,t)$ at a sufficient number of thermal stations along the length, an accurate description of the thermal loading components $BM_x(z,t)$, $BM_y(z,t)$, and $T_{sc}(z,t)$ can be ascertained by interpolation.

Linear Heat Flow

The sun's orientation at any thermal station z, defined by the angle $\psi(z,t)$, changes in time and causes a change in the heat flow around the circumference. If the temperature distribution is expressed as

$$\tilde{T}(s,z,t) = T_0 + T(s,z,t) \tag{10}$$

where T_0 is the steady-state mean absolute temperature and $T_0 \gg T(s,z,t)$ then letting $T = T(s,z,t)$ the equation of linear heat conduction and radiation can be written as

$$\frac{\partial^2 T}{\partial s^2} - \frac{\rho c}{K_T}\frac{\partial T}{\partial t} - \frac{4\sigma\epsilon T_0^3}{K_T h}T = \frac{\sigma\epsilon T_0^4 - \Upsilon}{K_T h} \tag{11}$$

where

$$\partial T/\partial s|_{s=0} = \partial T/\partial s|_{s=P} = 0 \tag{12}$$

and c, K_T, and ρ are the specific heat, thermal conductivity, and weight density of the material, and σ is the Stephan-Boltzmann constant.

The heat input $\Upsilon = \Upsilon(s,z,t)$ is proportional to the cosine of the angle between the surface normal and the direction of the thermal field. If the solar radiation intensity is given by J_s and if surface absorptivity and emissivity are given by α_s and ϵ, respectively, then the heat input can be ade quately described by

$$\Upsilon = \begin{cases} J_s\alpha_s\,\Xi\cos\left[\psi(z,t) - \dfrac{s}{r}+\dfrac{\phi}{2}\right] & 0\le s\le 2\pi r \\ \sigma\epsilon\alpha_s T_0^4 & 2\pi r < s \le P \end{cases} \tag{13}$$

where

$$\Xi = \begin{cases} 1 \text{ if } \cos[\psi(z,t) - (s/r) + (\phi/2)] > 0 \\ 0 \text{ if } \cos[\psi(z,t) - (s/r) + (\phi/2)] \le 0 \end{cases} \tag{14}$$

This function, identical to that used by Frisch[4] to study the static problem, leads to the prediction of temperature distributions which are in good agreement with those reported by Florio and Hobbs.[5]

The homogeneous part of Eq. (11) can be solved by separation of variables. This leads to a standard eigenvalue problem. The normalized thermal modes $T_n(s)$ and thermal-decay constants λ_n which are solutions to the eigenvalue problem can be used to express the solution to the nonhomogeneous equation in terms of a set of generalized thermal coordinates $q_n(z,t)$. That is, the solution may be written as

$$T(s,z,t) = \sum_{n=0}^{\infty} q_n(z,t)T_n(s) \tag{15}$$

where

$$d^2T_n(s)/ds^2 + (n\pi/P)^2T_n(s) = 0 \tag{16}$$

$$dq_n(z,t)/dt + \lambda_n q_n(z,t) = Q_n(z,t) \tag{17}$$

$$T_n(s) = \begin{cases} 1 & \text{for } n = 0 \\ 2^{1/2}\cos(n\pi/P)s & \text{for } n = 1,2,\ldots \end{cases} \tag{18}$$

$$\lambda_n = [4\sigma\epsilon T_0^3 + K_T h(n\pi/P)^2]/(\rho ch) \tag{19}$$

$$Q_n(z,t) = \frac{1}{\rho chP}\int_0^P [\Upsilon - \sigma\epsilon T_0^4]T_n(s)ds \tag{20}$$

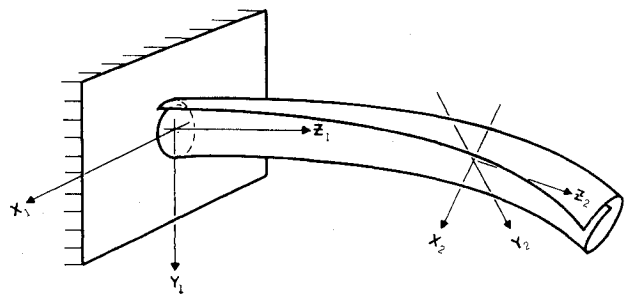

Fig. 3 Relative orientation of inertially fixed $[X_1,Y_1,Z_1]$ and local sliding $[X_2,Y_2,Z_2]$ coordinate systems.

Substitution of Eq. (15) into Eq. (10), and the result into the thermal-loading expressions given by Eqs. (3, 4, and 8), produces a series representation of the thermal-loading expressions in terms of the generalized thermal coordinates;

$$BM_x(z,t) = 2(2)^{1/2}e_cEhr^2P^2 \sin\frac{\phi}{2} \sum_{\substack{n=2 \\ n \text{ even}}}^{\infty} \frac{q_n(z,t)}{(n\pi r)^2 - P^2} \quad (21)$$

$$BM_y(z,t) = -2(2)^{1/2}e_cEhr^2P^2 \cos\frac{\phi}{2} \sum_{\substack{n=1 \\ n \text{ odd}}}^{\infty} \frac{q_n(z,t)}{(n\pi r)^2 - P^2} \quad (22)$$

$$T_{sc}(z,t) = 2(2)^{1/2}e_cEhrP \left\{ \sum_{\substack{n=1 \\ n \text{ odd}}}^{\infty} \frac{1}{n\pi} \times \left[\frac{n\pi Pre_s \cos\phi/2}{P^2 - (n\pi r)^2} - \frac{P}{n\pi} \right] \frac{\partial q_n(z,t)}{\partial \psi(z,t)} \right\} \frac{\partial \psi(z,t)}{\partial \varphi(z,t)} \frac{\partial \varphi(z,t)}{\partial z} \quad (23)$$

As the generalized thermal input $Q_n(z,t)$ is expressible as an analytic function of the relative sun orientation $\psi(z,t)$, the following expression is obtained for the derivative of $q_n(z,t)$ with respect to $\psi(z,t)$:

$$\frac{d}{dt}\left(\frac{\partial q_n(z,t)}{\partial \psi(z,t)}\right) + \lambda_n \left(\frac{\partial q_n(z,t)}{\partial \psi(z,t)}\right) = \frac{\partial Q_n(z,t)}{\partial \psi(z,t)} \quad (24)$$

Coordinate System

In order to describe the instantaneous position of the boom two coordinate systems are defined in a manner analogous to that used by Love[6]: one, the $[X_1,Y_1,Z_1]$ system inertially fixed at the clamped root of the cylinder, and another, the $[X_2,Y_2,Z_2]$ system sliding with unit velocity along the cylinder's strained longitudinal axis. The axes of the sliding coordinate system are always aligned along the cross-sectional principal axes of inertia having the directions shown in Figs. 2 and 3, and the components of curvature κ,κ' and twist τ of the strained longitudinal axis are the components of its angular-velocity vector resolved along the instantaneous positions of the $[X_2,Y_2,Z_2]$ system.

Let $[\mathbf{i}_1,\mathbf{j}_1,\mathbf{k}_1]$ be an orthonormal set of basis vectors fixed in and directed along the inertially fixed $[X_1,Y_1,Z_1]$ coordinate system.

Let $[\mathbf{i},\mathbf{j},\mathbf{k}]$ be an orthonormal set of basis vectors fixed at the centroid of the cross section at the root $z = 0$ and oriented so that they are parallel to the local $[X_2,Y_2,Z_2]$ axis system (Fig. 4).

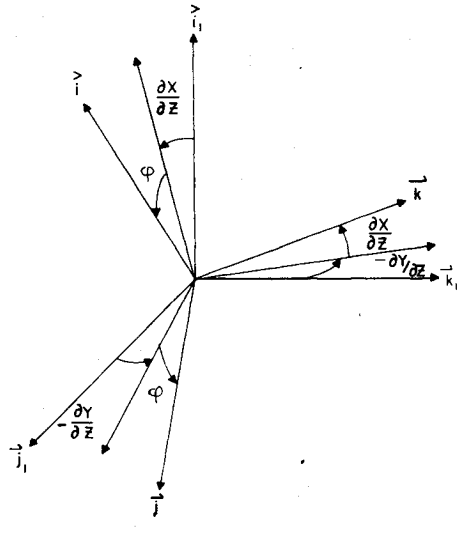

Fig. 4 Euler angle sequence used to relate the two sets of orthonormal basis vectors.

Let $[X(z,t),Y(z,t),z]$ define the coordinates of a point z at time t, along the longitudinal axis, relative to the fixed $[X_1,Y_1,Z_1]$ coordinate system.

If small-angle transverse bending is assumed, the transformation matrix becomes [where $X = X(z,t)$, $Y = Y(z,t)$ and $\varphi = \varphi(z,t)$]

$$\begin{Bmatrix} \mathbf{i} \\ \mathbf{j} \\ \mathbf{k} \end{Bmatrix} = \begin{bmatrix} \cos\varphi & \sin\varphi & -\frac{\partial X}{\partial z}\cos\varphi - \frac{\partial Y}{\partial z}\sin\varphi \\ -\sin\varphi & \cos\varphi & \frac{\partial X}{\partial z}\sin\phi - \frac{\partial Y}{\partial z}\cos\varphi \\ \frac{\partial X}{\partial z} & \frac{\partial Y}{\partial z} & 1 \end{bmatrix} \begin{Bmatrix} \mathbf{i}_1 \\ \mathbf{j}_1 \\ \mathbf{k}_1 \end{Bmatrix} \quad (25)$$

The components of curvature, κ,κ' relative to the local axis system are

$$\kappa = -(\partial^2 Y/\partial z^2)\cos\varphi + (\partial^2 X/\partial z^2)\sin\varphi \quad (26)$$

$$\kappa' = (\partial^2 Y/\partial z^2)\sin\varphi + (\partial^2 X/\partial z^2)\cos\varphi \quad (27)$$

The twist is

$$\tau = \partial\varphi/\partial z \quad (28)$$

Equation of Elastic Equilibrium

Landau and Lifschitz,[7] and Love[6] show that the equations of elastic equilibrium relative to the local $[X_2,Y_2,Z_2]$ coordinate system can be written as

$$d\mathbf{V}/dz + \mathbf{F} = 0 \quad (29)$$

$$d\mathbf{M}/dz + \mathbf{k} \times \mathbf{V} + \mathbf{K} = 0 \quad (30)$$

where $\mathbf{V}$ is the resultant of the internal stress and $\mathbf{M}$ its moment about the centroid of the cross section. $\mathbf{F}$ is the resultant of the applied force and $\mathbf{K}$ is its resultant couple measured per unit length.

By neglecting tension, deleting terms which are of second order in displacement, and using the notation of Love,[6] we write

$$\mathbf{V} = N\mathbf{i} + N'\mathbf{j},\ \mathbf{M} = G\mathbf{i} + G'\mathbf{j} + H\mathbf{k} \quad (31)$$

$$\mathbf{F} = F_1\mathbf{i} + F_2\mathbf{j},\ \mathbf{K} = K\mathbf{i} + K'\mathbf{j} + \Theta\mathbf{k} \quad (32)$$

(N,N' are the "shearing forces," G,G' are the "flexural couples," and H is the "torsional couple") substitute into the equations of equilibrium, and find that

$$[(dN/dz) + F_1]\mathbf{i} + [(dN'/dz) + F_2]\mathbf{j} = 0 \quad (33)$$

$$[(dG/dz) - N' + K]\mathbf{i} + [(dG'/dz) + N + K']\mathbf{j} + [(dH/dz) + \Theta]\mathbf{k} = 0 \quad (34)$$

From the Bernoulli-Euler assumption of elementary strength of materials, and Timoshenko's theory of members of open section, the flexural and torsional couples are related to the components of curvature and twist by the following:

$$G = EI\kappa,\ G' = EI\kappa' \quad (35)$$

$$H = -C_w\partial^2\tau/\partial z^2 + C_T\tau \quad (36)$$

where EI is the average bending stiffness, C_w is the warping rigidity, and C_T is the torsional rigidity. Directly substituting Eqs. (26–28) into Eqs. (35) and (36) and the resulting expressions into Eqs. (33) and (34), upon deletion of second-order terms we have

$$EI\frac{\partial^4 X}{\partial z^4} + \left(\frac{\partial K'}{\partial z} - F_1\right)\cos\varphi + \left(\frac{\partial K}{\partial z} + F_2\right)\sin\varphi = 0 \quad (37)$$

$$EI\frac{\partial^4 Y}{\partial z^4}+\left(\frac{\partial K'}{\partial z}-F_1\right)\sin\varphi-\left(\frac{\partial K}{\partial z}+F_2\right)\cos\varphi=0 \quad (38)$$

$$-C_w(\partial^4\varphi/\partial z^4)+C_T(\partial^2\varphi/\partial z^2)+\Theta=0 \quad (39)$$

For the practical analysis of actual flight quality booms EI, C_T, and C_w are best measured experimentally. This has been done for the numerical results presented.

Disturbance Forces

The disturbance forces of interest to this study are: 1) the body forces associated with the translational and rotational acceleration of all mass elements along the length; 2) the dissipative forces associated with viscoelastic damping of transverse and torsional motion; and 3) the thermal loading due to solar radiation. All other disturbance forces existing in flight (solar pressure, aerodynamic drag, gravitational effects, etc.) will be ignored.

The three disturbance forces cited can be expressed simply as

$$\mathbf{F}=0 \quad (40)$$

$$\mathbf{K}=\mathbf{K}_B+\mathbf{K}_D+\mathbf{K}_T \quad (41)$$

where $\mathbf{K}_B$, $\mathbf{K}_D$, and $\mathbf{K}_T$ are the resultant couple distributions associated with the body forces, the dissipative forces, and the thermal loading, respectively.

The booms to be studied may be extremely long, and the standard small-angle bending assumptions cannot be applied to determine the body forces. (That is, when the instantaneous deflected shape of the boom and the direction of acceleration of each mass element along it are accounted for, the resultant couple distribution $\mathbf{K}_B$ has a significant component caused by nonplanar motion about an axis normal to the cross section which couples bending into torsional motion.)

At time t, the point z' along the longitudinal axis can be defined by the vector $\mathbf{R}(z',t)$ where

$$\mathbf{R}(z',t)=X(z',t)\mathbf{i}_1+Y(z',t)\mathbf{j}_1+z'\mathbf{k}_1 \quad (42)$$

The element at z' has mass $\rho hP/g dz'$ and rotational inertia $I_s dz'$ about the axis of shear centers. The couple at z resulting from the kinetic reactions of all accelerating mass elements between z and the boom tip is

$$\mathbf{K}_B=-\frac{d}{dz}\left\{\int_L^z[\mathbf{R}(z',t)-\mathbf{R}(z,t)]\times\frac{\rho hP}{g}\frac{\partial^2\mathbf{R}(z',t)}{\partial t^2}dz'+\int_L^z I_s\frac{\partial^2\varphi(z',t)}{\partial t^2}\mathbf{k}(z')dz'\right\} \quad (43)$$

where $\mathbf{k}(z')$ is the unit vector normal to the cross section at z'.

Substitution of Eq. (42) into (43), transforming into the [i,j,k] reference system, differentiation, and deletion of second-order terms yields

$$\mathbf{K}_B=-\frac{\rho hP}{g}\int_L^z\left\{\left[\frac{\partial^2 Y(z',t)}{\partial t^2}\cos\varphi(z,t)-\frac{\partial^2 X(z',t)}{\partial t^2}\sin\varphi(z,t)\right]\mathbf{i}-\left[\frac{\partial^2 Y(z',t)}{\partial t^2}\sin\varphi(z,t)+\frac{\partial^2 X(z',t)}{\partial t^2}\cos\varphi(z,t)\right]\mathbf{j}\right\}dz'+\frac{\rho hP}{g}\left\{\int_L^z(z'-z)\times\left[\frac{\partial^2 X(z,t)}{\partial z^2}\frac{\partial^2 Y(z',t)}{\partial t^2}-\frac{\partial^2 Y(z,t)}{\partial z^2}\frac{\partial^2 X(z',t)}{\partial t^2}\right]dz'-I_s\frac{\partial^2\varphi(z,t)}{\partial t^2}\right\}\mathbf{k} \quad (44)$$

The $\mathbf{k}$ component of $\mathbf{K}_B$ obviously contains a term which couples bending into torsion. This term is insignificant for cylinders which are torsionally stiff or of short length; however, for cylinders of long length and low torsional rigidity, it cannot be neglected. Analogous terms (not shown) are also present in the $\mathbf{i}$ and $\mathbf{j}$ components of $\mathbf{K}_B$. They are neglected in Eq. (44) since their effects have been found to be nearly zero for the problems of interest.

The transverse and torsional dissipative forces are actually a combination of structural, viscous, and coulomb damping effects. Furthermore, reported test data given by Predmore[8] show that so-called identical flight-quality booms have transverse-damping characteristics which may differ by as much as two orders of magnitude. Although no data has been published describing torsional-damping characteristics, such damping is strongly influenced by the frictional contact between overlapping surfaces and can eliminate all initially induced torsional motion in just a few cycles of vibration. It has therefore been decided for this analysis to describe damping by two independent equivalent viscous damping coefficients β_x and β_φ which control the damping of transverse and torsional motion, respectively. The couple distribution $\mathbf{K}_D$ associated with the dissipative forces is approximated by

$$\mathbf{K}_D=-\beta_x\int_L^z\left[\frac{\partial Y(z',t)}{\partial t}\cos\varphi(z,t)-\frac{\partial X(z',t)}{\partial t}\sin\varphi(z,t)\right]dz'\,\mathbf{i}+\beta_x\int_L^z\left[\frac{\partial Y(z',t)}{\partial t}\sin\varphi(z,t)+\frac{\partial X(z',t)}{\partial t}\cos\varphi(z,t)\right]dz'\,\mathbf{j}-\beta_\varphi\frac{\partial\varphi(z,t)}{\partial t}\mathbf{k} \quad (45)$$

The resultant couple distribution $\mathbf{K}_T$ associated with thermal loading can be derived from the work previously presented. By defining a sufficient number of thermal stations to solve the generalized thermal-coordinate Eqs. (17) and (24), the thermal loading can be obtained at every point along the boom by interpolation. Because the components of the thermal load are derived relative to the local $[X_2,Y_2,Z_2]$ axis system, the reversed thermal reaction $\mathbf{K}_T$ is [where $BM_x=BM_x(z,t)$, $BM_y=BM_y(z,t)$, and $T_{sc}=T_{sc}(z,t)$]

$$\mathbf{K}_T=-(\partial BM_x/\partial z)\mathbf{i}-(\partial BM_y/\partial z)\mathbf{j}-(\partial T_{sc}/\partial z)\mathbf{k} \quad (46)$$

Equation of Thermally Induced Vibration

The resultant couple distribution $\mathbf{K}$ is obtained by vector addition of Eqs. (44–46), the [i,j,k] components of which define K,K', and Θ, respectively. Substitution of these components, along with those associated with the resultant-force distribution $\mathbf{F}$ given by Eq. (40), into Eqs. (37–39) yield the equations of thermally induced vibration [where $c\varphi=\cos\varphi(z,t)$ and $s\varphi=\sin\varphi(z,t)$]

$$EI\frac{\partial^4 X}{\partial z^4}+\frac{\rho hP}{g}\frac{\partial^2 X}{\partial t^2}+\beta_x\frac{\partial X}{\partial t}=\frac{\partial^2}{\partial z^2}[BM_y c\varphi+BM_x s\varphi] \quad (47)$$

$$EI\frac{\partial^4 Y}{\partial z^4}+\frac{\rho hP}{g}\frac{\partial^2 Y}{\partial t^2}+\beta_x\frac{\partial Y}{\partial t}=\frac{\partial^2}{\partial z^2}[BM_y s\varphi-BM_x c\varphi] \quad (48)$$

$$C_w\frac{\partial^4\varphi}{\partial z^4}-C_T\frac{\partial^2\varphi}{\partial z^2}+I_s\frac{\partial^2\varphi}{\partial t^2}+\beta_\varphi\frac{\partial\varphi}{\partial t}=-\frac{\partial T_{sc}}{\partial z}+\frac{\rho hP}{g}\int_L^z(z'-z)\left[\frac{\partial^2 X(z,t)}{\partial z^2}\frac{\partial^2 Y(z',t)}{\partial t^2}-\frac{\partial^2 Y(z,t)}{\partial z^2}\frac{\partial^2 X(z',t)}{\partial t^2}\right]dz' \quad (49)$$

These equations define the boom's response in a directional thermal field; the boundary conditions are therefore time-dependent. If the boom is clamped in two-axis bending and torsion at the root, and free to deflect and warp at the tip, the time-dependent boundary conditions are, at $(0,t)$

$$X = Y = \varphi = 0 \tag{50}$$

$$\partial X/\partial z = \partial Y/\partial z = \partial\varphi/\partial z = 0 \tag{51}$$

and, at (L,t)

$$EI\partial^2 X/\partial z^2 = BM_y \cos\varphi + BM_x \sin\varphi \tag{52}$$

$$EI\partial^2 Y/\partial z^2 = BM_y \sin\varphi - BM_x \cos\varphi \tag{53}$$

$$\partial^2\varphi/\partial z^2 = 0 \tag{54}$$

$$EI(\partial^3 X/\partial z^3) = (\partial/\partial z)[BM_y \cos\varphi + BM_x \sin\varphi] \tag{55}$$

$$EI(\partial^3 Y/\partial z^3) = (\partial/\partial z)[BM_y \sin\varphi - BM_x \cos\varphi] \tag{56}$$

$$C_w(\partial^3\varphi/\partial z^3) - C_T\partial\varphi/\partial z = -T_{sc} \tag{57}$$

These equations and boundary conditions are consistent with the thermostress analysis of Boley and Wiener.[2,9] Recent work done by Jordan[10] shows that, strictly speaking, the right-hand side of Eq. (54) is nonzero if there is warping deformation due to thermal strain. However for booms of practical interest, the effect of this discrepancy is small.

Solution to Thermally Induced Vibration Equations

Following the methods presented by Mindlin and Goodman[11] for solving equations with time-dependent boundary conditions, we define the coordinates $X_s = X_s(z,t)$, $Y_s = Y_s(z,t)$, and $\varphi_s = \varphi_s(z,t)$ as those of the instantaneous thermal-equilibrium position of the boom (that is, the position it would assume in the directional thermal field if all the body and dissipative forces were set equal to zero). These coordinates satisfy Eqs. (52, 53, and 57), respectively, and all the stated boundary conditions (50–57).

Let $x_n(z)$, $y_n(z)$, and $\varphi_n(z)$ be the undamped unforced transverse and torsional modes of vibration which satisfy the equations

$$EI[d^4x_n(z)/dz^4] - (\rho hP/g)\omega_{x_n}{}^2 x_n(z) = 0 \tag{58}$$

$$EI[d^4y_n(z)/dz^4] - (\rho hP/g)\omega_{x_n}{}^2 y_n(z) = 0 \tag{59}$$

$$C_w \frac{d^4\varphi_n(z)}{dz^4} - C_T \frac{d^2\varphi_n(z)}{dz^2} - I_s\omega_{\varphi_n}{}^2\varphi_n(z) = 0 \tag{60}$$

and also satisfy the time-independent parts of the stated boundary conditions.

At each instant of time, the coordinates of the thermal-equilibrium position are known; $X_s(z,t)$, $Y_s(z,t)$, and $\varphi_s(z,t)$ may therefore be expressed as series expansions,

$$X_s(z,t) = \sum_{n=1}^{\infty} \alpha_n(t)x_n(z) \tag{61}$$

$$Y_s(z,t) = \sum_{n=1}^{\infty} \beta_n(t)y_n(z) \tag{62}$$

$$\varphi_s(z,t) = \sum_{n=1}^{\infty} \gamma_n(t)\varphi_n(z) \tag{63}$$

If a solution of the form

$$X(z,t) = X_s(z,t) + \sum_{n=1}^{\infty} a_n(t)x_n(z) \tag{64}$$

$$Y(z,t) = Y_s(z,t) + \sum_{n=1}^{\infty} b_n(t)y_n(z) \tag{65}$$

$$\varphi(z,t) = \varphi_s(z,t) + \sum_{n=1}^{\infty} c_n(t)\varphi_n(z) \tag{66}$$

is assumed for the thermally induced-vibration equations the generalized displacement coordinates $A_n(t)$,$B_n(t)$,$C_n(t)$ are the solution to the equations

$$\frac{d^2A_n(t)}{dt^2} + 2\zeta_x\omega_{x_n}\frac{dA_n(t)}{dt} + \omega_{x_n}{}^2[A_n(t) - \alpha_n(t)] = 0 \tag{67}$$

$$\frac{d^2B_n(t)}{dt^2} + 2\zeta_x\omega_{x_n}\frac{dB_n(t)}{dt} + \omega_{x_n}{}^2[B_n(t) - \beta_n(t)] = 0 \tag{68}$$

$$\frac{d^2C_n(t)}{dt^2} + 2\zeta_\varphi\omega_{\varphi n}\frac{dC_n(t)}{dt} + \omega_{\varphi n}{}^2[C_n(t) - \gamma_n(t)] = C_n{}^*(t) \tag{69}$$

where

$$C_n{}^*(t) = +\frac{1}{I_sL}\int_0^L \varphi_n(z)\int_L^z \frac{\rho hP}{g}(z' - z) \times \left[\frac{\partial^2 X(z,t)}{\partial z^2}\frac{\partial^2 Y(z',t)}{\partial t^2} - \frac{\partial^2 Y(z,t)}{\partial z^2}\frac{\partial^2 X(z',t)}{\partial t^2}\right] dz'dz \tag{70}$$

$$\beta_x = 2(\rho hP/g)\zeta_x\omega_{x_n} \tag{71}$$

$$\beta_\varphi = 2I_s\zeta_\varphi\omega_{\varphi n} \tag{72}$$

and $A_n(t) = a_n(t) + \alpha_n(t)$, $B_n(t) = b_n(t) + \beta_n(t)$, and $C_n(t) = c_n(t) + \gamma_n(t)$.

If the generalized force $C_n{}^*(t)$ can be approximated by the first mode's transverse motion, then it can be shown that

$$C_n{}^*(t) = \left[A_1(t)\frac{d^2B_1(t)}{dt^2} - B_1(t)\frac{d^2A_1(t)}{dt^2}\right]P_n \tag{73}$$

where

$$P_n = \frac{\rho hP}{I_sLg}\int_0^L \varphi_n(z)\int_L^z (z' - z)\frac{d^2x_1(z)}{dz^2}y_1(z')dz'dz \tag{74}$$

One fact which becomes apparent from the generalized displacement-coordinate Eqs. (67–69) is that the elastic spring or restoring force is measured not from the undeflected position of the boom, but from the time-varying position of thermal-equilibrium. This, of course, is physically evident.

Nominal Model

The nominal model for the results presented is the boom used on OGO-IV and many other existing satellites. These results should provide a heuristic understanding of the basic mechanism behind thermally induced vibrations and the effect of changes in various parameters on its magnitude. The parameters studied are those which can be controlled by a manufacturer and used to govern the amplitude and stability of motion. Nominal magnitudes used to describe the boom's geometrical and physical properties are shown in Table 1.

For all runs presented, the boom is assumed to be initially in an unstrained state at uniform ambient-temperature. The sun is assumed to be turned on at time zero, and its orientation remains fixed in time along the inertially fixed negative Y_1 axis. Throughout the ensuing dynamic response, the thermal input at all thermal stations is assumed to be that of one sun normal to the strained longitudinal axis.

Effect of Thermal Torque

Recent unpublished test data obtained by R. Predmore and C. Staugaitis[12] at NASA/GSFC have been used by Frisch[13] to check theoretical predictions. Results indicate that the torsional response due to thermal torque can be reasonably well-predicted. More experimental work is needed, however, before a more positive statement can be justified.

Table 1 Nominal magnitudes for boom

Boom material	=	beryllium copper silver plated (polished)
Boom length	=	$L = 60$ ft
Perimeter of cross section	=	$P = 2$ in.
Total overlap angle	=	$\phi = 90°$
Wall thickness	=	$h = 0.002$ in.
Weight density of material	=	$\rho = 0.2714$ lb/in.^{3}
Young's modulus	=	$E = 0.19 \times 10^8$ lb/in.^{2}
Bending stiffness	=	$EI = 16.6$ lb ft^2
Damping ratio for torsion	=	$\zeta_\varphi = 0.2$
Damping ratio for bending	=	$\zeta_x = 0.005$
Torsional rigidity	=	$C_T = 0.05$ lb-in.^{2}
Warping rigidity	=	$C_w = 1700$ lb-in.^{4}
Thermal conductivity	=	$K_T = 4.167$ Btu/(hr-in.-°F)
Specific heat	=	$c = 0.1$ Btu/(lb-°F)
Solar radiation intensity	=	$J_s = 3.065$ Btu/(hr-in.^{2})
Thermal expansion coefficient	=	$e_c = 0.104 \times 10^{-4}$ in./(in.-°F)
Emissivity	=	$\epsilon = 0.035$
Absorptivity	=	$\alpha_s = 0.13$
Stephan-Boltzmann constant	=	$\sigma = 0.121 \times 10^{-10}$ Btu/(hr-in.^{2})

Keeping in mind the possibility of some inadequacy in any representation of thermal torque, we began a qualitative analysis of it by making several computer runs to determine the effect of changes in initial sun orientation, damping, and the inclusion of the first three torsional modes of vibration.

For small-angle torsional motion, thermal torque has the effect of introducing into the system a negative torsional spring which effectively decreases the system's torsional rigidity. This decrease in torsional rigidity causes an increase in the amplitude of the torsional response. Heat can flow only at a finite rate; increasing the amplitude of the torsional response therefore causes an averaging of the temperature distribution and hence a decrease in the thermal loading. This in effect limits the amplitude of the transverse motion.

The results presented in Ref. 13 are actually more complex, but tend to agree with this basic generalization. Worst-case results are obtained for the particular sun orientation where the magnitude of thermal torque is a minimum. Thermal torque can have a stabilizing effect upon transverse motion, but for worst-case results it should be deleted from the analysis. This is done for all succeeding runs, which show that—with the effect of thermal torque deleted—it is still possible to demonstrate that transverse thermally induced vibrations can occur, and furthermore that the predicted amplitudes are reasonably close to those deducible from existing flight data.

Numerical Results with Effect of Thermal Torque Deleted

Each of the succeeding figures illustrates the change in the boom's dynamic response as a function of time. This is achieved by introducing the oblique (time) axis and allowing the origin of the coordinate system in which tip deflection is measured to simply translate without rotating along the time axis at a constant rate. The motion shown is only that of the tip's actual position; the position of thermal equilibrium (to be referred to) toward which the boom is continually moving is not shown. The discussion will show that, when the position of thermal equilibrium changes with a strong component at or near the first natural bending frequency, an unstable thermally induced transverse oscillation can be excited; furthermore, when the position of thermal equilibrium changes at any other frequency (for example, the first torsional frequency), unstable transverse motion will not occur. It should be further noted that in several examples the predicted amplitudes exceed the limits of small-angle deflection theory. However, since the numerical results do agree, in a phenomenological sense, with satellite data, the effects of including neglected terms would probably change the numerical values of the answers but not the basic characteristics of the motion.

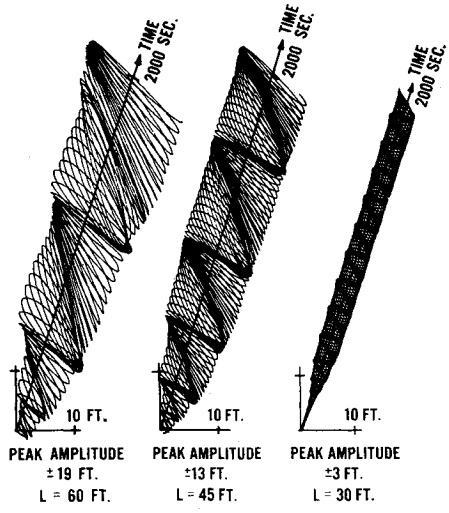

Fig. 5 Effect of boom length on thermally induced vibrations. Tip motion of 60, 45, and 30 ft booms when placed in sunlight at time zero.

Figure 5 shows the effect of boom length upon the response of the nominal model. For the time spans shown, the 60-, 45-, and 30-ft booms exhibit thermally induced motion. The vibration amplitudes shown are consistent with data obtained from the flights of the OGO-IV and OGO-V spacecraft: that is, the 60-ft electron probe on OGO-IV is believed to oscillate with an amplitude of ±20 ft, and the 30-ft electron probes on OGO-V are believed to oscillate with an amplitude of ±2 ft.

Figure 6 shows the effect of the boom's transverse damping ratio. If this parameter could be easily controlled and significantly increased above its nominal value of 0.005, the amplitude of the thermally induced vibration could be stabilized, or at least limited to an acceptable magnitude. Various manufacturers have attempted to increase the boom's transverse damping characteristics by coating the surface with thin viscoelastic laminae; however, the experimental work reported in Ref. 8 shows that these attempts have been essentially unsuccessful.

Figure 7 illustrates the observation that, for large-amplitude thermally induced transverse motion to exist, the boom

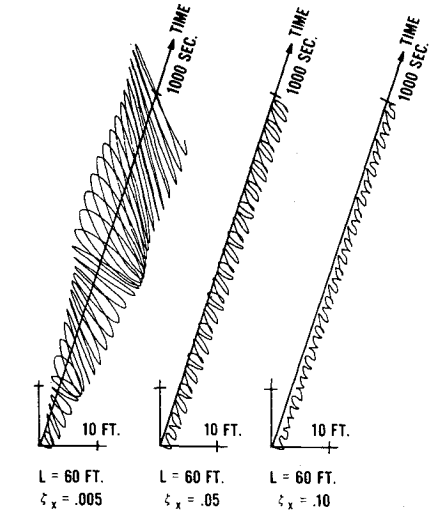

Fig. 6 Effect of transverse damping on thermally induced vibrations. Tip motion of 60 ft boom with $\zeta_x = 0.005$, 0.05, and 0.10 when placed in sunlight at time zero.

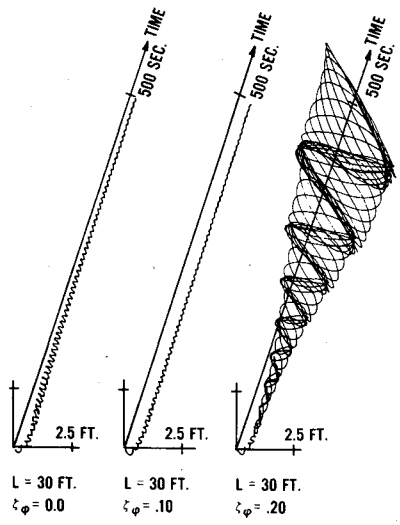

Fig. 7 Effect of torsional damping on thermally induced vibrations. Tip motion of 30 ft boom with $\zeta_\varphi = 0, 0.10$, and 0.20 when placed in sunlight at time zero.

must respond torsionally at or near the first natural bending frequency ω_{x_1}. This in effect causes the position of thermal equilibrium to move at ω_{x_1}, and hence to drive the boom at its resonant frequency.

Equation (71) shows that, with the effect of thermal torque deleted by setting $\gamma_n(t) = 0$, the torsional response depends upon the magnitude of the torsional damping ratio, ζ_φ, and the nonlinear generalized force $C_n^*(t)$. The fact that $C_n^*(t)$ depends upon the boom's actual position and its position of thermal equilibrium leads to results which are extremely complex. A judicious choice of example, however, can clearly illustrate the aforementioned observation. Accordingly, Fig. 7 shows how the resultant response of a nominal 30-ft boom differs for the torsional damping ratios 0, 0.1, and 0.2, respectively.

In Fig. 7 for $\zeta_\varphi = 0$, from time zero, the torsional response (not shown) at the boom tip gradually builds up at the first torsional frequency ω_{φ_1} to an amplitude of about $\pm 5\pi$ rad at 500 sec. This has the dual effect of causing the position of thermal equilibrium to change at about ω_{φ_1} and of causing an averaging of the temperature distribution. The figure shows both effects. Because the position of thermal equilibrium changes at the frequency ω_{φ_1}, the effective thermal loading acts as a high-frequency forcing function which has only a slight effect on the transverse motion and cannot excite an unstable oscillation. The effect of temperature averaging appears in that the curve shown is closer to the time axis after the transient response than during it. For the second curve $\zeta_\varphi = 0.1$, the amplitude of the torsional response achieved during the initial thermal transient (not shown) is found to gradually decay to zero at a nonresonant frequency; the transverse motion gradually damps out to a displaced position, that of static thermal equilibrium. For the third curve $\zeta_\varphi = 0.2$, the torsional response (not shown) is found to build up gradually at the first transverse bending frequency ω_{x_1} to a steady-state amplitude of about $\pm 3\pi$ rad. As the position of thermal equilibrium depends upon the torsional response, it too will change at about ω_{x_1}. The result is to drive the system near resonance and to excite large-amplitude thermally induced transverse vibrations.

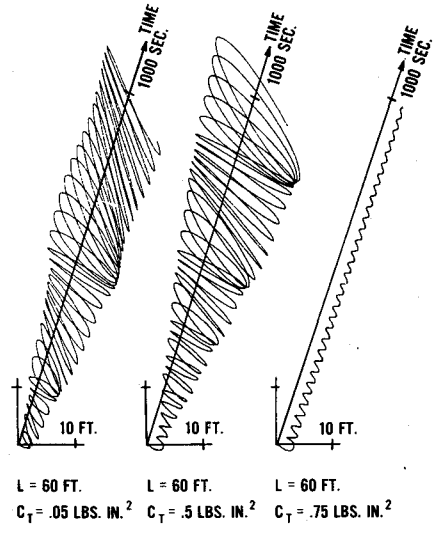

Fig. 8 Effect of torsional rigidity on thermally induced vibrations. Tip motion of 60 ft boom with $C_T = 0.05, 0.5$, and 0.75 lb-in.^{2} when placed in sunlight at time zero.

Figure 8 contains curves which indicate a practical means of designing a deployable boom which will be stable in direct sunlight. The curves show the effect of varying the antenna's torsional rigidity. The first curve shows the response of the nominal 60-ft boom, which is obviously unstable; in the second curve, the torsional rigidity is increased by a factor of 10 to 0.5 lb-in.^{2}. The slight increase in the response amplitude shows that, as the torsional response (not shown) has been reduced by nearly a factor of 10 in amplitude, the effect on temperature averaging of large-angle torsional motion has also been reduced, with a corresponding increase in the effective loading. In the third curve, the torsional rigidity is increased above its nominal value by a factor of 15 to 0.75 lb-in.^{2}. Here the amplitude of the torsional motion has been reduced to the point where it no longer has an effect upon the position of thermal equilibrium. The resulting transverse motion, as shown is stable.

Various manufacturers have used this idea and have submitted flight-quality booms to NASA/GSFC for evaluation; all the booms submitted have the seams of the open-section cylinder zippered in various ways. Each of these designs exhibits a torsional rigidity at least 1500 times greater than that of the nominal model defined, and about 100 times greater than needed to achieve stability.

Both RAE (Radio Astronomy Explorer), launched September 1968 and OGO VI (Orbiting Geophysical Observatory) launched June 1969, use the zippered-boom concept. As predicted the four 750-ft-long booms on RAE and the two 30-ft booms on OGO-VI are stable in and out of sunlight.

Conclusions

1) The thermally induced-vibration theory presented here explains the anomalous spacecraft motion observed on several three-axis-stabilized satellites deploying long torsionally weak thin-walled cylinders of open section in direct sunlight.

2) The problem of designing a thermally stable deployable boom can be solved by zippering the seam of the open-section cylinder so as to increase its torsional rigidity by several orders of magnitude.

3) Any three-axis-stabilized satellite which requires long booms and geometric stability should not use torsionally weak thin-walled cylinders of open section.

References

[1] *Proceedings of the Symposium on Gravity-Gradient Attitude Control*, U.S. Air Force and Aerospace Corp., Dec. 1968, SAMSO-TR-69-307, pp. 3-1 to 3-52 and 7-1 to 7-17.

[2] Boley, B. A. and Weiner, J. H., *Theory of Thermal Stresses*, Wiley, New York, 1960.

[3] Timoshenko, S., "Theory of Bending, Torsion and Buckling of Thin Walled Members of Open Section," *Journal of the Franklin Institute*, Vol. 239, Nos. 3 and 4, 1945, pp. 201–219, 249–268.

[4] Frisch, H. P., "Thermal Bending Plus Twist of a Thin-Walled Cylinder of Open Section With Application to Gravity-Gradient Booms," TN D-4069, Aug. 1967, NASA.

[5] Florio, F. A. and Hobbs, R. B., "An Analytical Representation of Temperature Distributions in Gravity-Gradient Rods," *AIAA Journal*, Vol. 6, No. 1, Jan. 1968, pp. 99–102.

[6] Love, A. E. H., *The Mathematical Theory of Elasticity*, Dover, New York, 1944.

[7] Landau, L. D. and Lifschitz, E. M., *Theory of Elasticity*, Addison-Wesley, Reading, Mass., 1959.

[8] Predmore, R., Staugaitis, C., and Jellison, "Damping Behavior of DeHavilland Stem Booms," TN D-3996, June 1967, NASA.

[9] Boley, B. A., "Thermally Induced Vibrations of Beams," *Journal of the Aeronautical Sciences*, Vol. 23, No. 2, Feb. 1956, pp. 179–181.

[10] Jordan, P. F., "Observations on the Mechanisms of Thermal Torque Instability" *ASME/AIAA 10th Structures, Structural Dynamics and Materials Conference*, AIAA, New York, 1969.

[11] Mindlin, R. D. and Goodman, L. E., "Beam Vibration with Time-Varying Boundary Conditions," *Journal of Applied Mechanics*, Vol. 17, Dec. 1950, pp. 377–380.

[12] Predmore, R. E. and Staugaitis, C. L., private communications, Feb. 1969.

[13] Frisch, H. P., "Coupled Thermally Induced Transverse Plus Torsional Vibrations of a Thin-Walled Cylinder of Open Section," TR R-333, March 1970, NASA.

AUGUST 1970 J. SPACECRAFT VOL. 7, NO. 8

Buoyant Venus Station Requirements

STANLEY R. SADIN* AND RONALD E. FRANK†
Martin Marietta Corporation, Denver, Colo.

Use of a Buoyant Venus Station, a balloon-supported instrument package, to explore in the atmosphere of Venus would permit instruments to operate in a moderate environment with advantages of long duration in the atmosphere and mobility. Measurements relating to atmosphere and surface could be made, the latter either indirectly or by sondes dropped from the station. The concept is not sensitive to the choice of companion spacecraft mission mode; with minor differences, a station weighing 500 lb at deployment is suitable for flyby, orbital, and swingby missions. This paper describes three technologies requiring development: heat shield, superpressure balloon, and tracking of the station to determine position. A modest development program is proposed.

Nomenclature

A	=	area, ft^2
B	=	ballistic coefficient, slug/ft^2
C	=	coefficient, nondimensional
DSIF	=	Deep Space Information Facility
DSN	=	Deep Space Network
h	=	height, ft
M	=	Mach number, dimensionless
$\dot{q}$	=	heating rate, Btu/ft^2-sec
q	=	dynamic pressure, lb/ft^2
r	=	radius, ft
SE	=	sub-Earth point, dimensionless
SWR	=	Southwestern Research Corporation
t	=	Time, sec
T	=	Temperature, °R
UHF	=	ultra-high frequency, dimensionless
v	=	velocity, fps
V	=	volume, ft^3
ρ	=	density, lb/ft^3

Subscripts

B	=	balloon
D	=	drag
E	=	entry

Presented as Paper 69-1068 at the AIAA 6th Annual Meeting and Technical Display, Anaheim, Calif., October 20–24, 1969; submitted November 3, 1969; revision received March 26, 1970. Work supported by NASA under Contracts NAS1-6607 and NAS1-7590.

* Director, Research and Development.
† Project Engineer, Venus Program.

Introduction

THE use of a buoyant station[1,2] to explore in the atmosphere of Venus has been under study since 1966. By drifting with the prevailing winds for periods of one week to possibly several months, this vehicle could answer many scientific questions that cannot be easily answered by any other type vehicle such as a ballistic probe. What is the atmospheric circulation pattern and the mechanism driving it? What is the composition and structure of those mysterious clouds? What are the trace elements in the predominant CO_2 atmosphere? What is the structure of the clouds? What is the general topography of the surface (determined by mapping from the station)? The Buoyant Venus Station (BVS) permits instruments to be supported in the atmosphere in a moderate environment with the additional advantages of long-duration survival and mobility over the surface generated by existing winds. A typical complement of instruments would include radar altimeter, pressure, and temperature transducers, photometers, water vapor detector, accelerometers, mass spectrometer/gas chromatograph, and possibly some simple life-detection equipment. A cable suspended from the station supports the temperature and water vapor instruments. The below-station atmosphere is sensed by drop sondes, which relay their data to the station. The drifting station may either relay its data to a companion orbiting spacecraft or directly to Earth. Balloon technology, though adequate for Earth-launched balloons, requires further development for this application. The ability to track the station as it moves across the planet surface appears to present measurement technique and accuracy problems. Studies are being conducted on balloon-based